Growth rate and the cutoff wavelength of the Darrieus-Landau instability in laser ablation

Mikhail Modestov, Vitaly Bychkov, Damir Valiev, and Mattias Marklund
Department of Physics, Umeå University, 901 87 Umeå, Sweden

(Received 6 May 2009; revised manuscript received 30 July 2009; published 14 October 2009)

The main characteristics of the linear Darrieus-Landau instability in the laser ablation flow are investigated. The dispersion relation of the instability is found numerically as a solution to an eigenvalue stability problem, taking into account the continuous structure of the flow. The results are compared to the classical Darrieus-Landau instability of a usual slow flame. The difference between the two cases is due to the specific features of laser ablation: sonic velocities of hot plasma and strong temperature dependence of thermal conduction. It is demonstrated that the Darrieus-Landau instability in laser ablation is much stronger than in the classical case. In particular, the maximum growth rate in the case of laser ablation is about three times larger than that for slow flames. The characteristic length scale of the Darrieus-Landau instability in the ablation flow is comparable to the total distance from the ablation zone to the critical zone of laser light absorption. The possibility of experimental observations of the Darrieus-Landau instability in laser ablation is discussed.

DOI: 10.1103/PhysRevE.80.046403 PACS number(s): 52.35.Py, 52.57.Fg, 52.38.Mf

I. INTRODUCTION

Inertial confinement fusion (ICF) is believed to be one of the promising energy sources in the 21st century. The aim of ICF is to compress a plasma target to densities and temperatures high enough to trigger a thermonuclear reaction. Despite a great technical development and progress in power supplies during last decades [1], hydrodynamic instabilities remain the limiting factor in fusion performance and efficiency. In this respect, the most difficult obstacle in achieving ICF is the Rayleigh-Taylor (RT) instability, which arises because of target acceleration [2–9]. Still, the RT instability is not the only instability of importance in ICF; for example, the laser generated plasma is also subjected to the so called Darrieus-Landau (DL) instability [5,10–17]. Traditionally, the DL instability is known as the hydrodynamic instability of a slow flame [18–21], which makes the flame front corrugated and increases the burning rate. Flame is the most typical example of a deflagration wave, which is a front propagating due to energy release and thermal conduction. Other interesting examples of deflagration come from astrophysical applications like the big bang model and type I supernovae [22–27]. The ablation flow generated by laser radiation on a plasma target is also a deflagration wave [9,28,29]. On the basis of similar physical properties of deflagrations, one should expect the DL instability to develop in laser ablation. The purpose of the present theoretical work is to answer some of the key questions concerning the DL instability in laser ablation and to indicate conditions for experimental observation of the instability.

The flow generated by a slow flame is almost incompressible, which is taken into account in the classical theory of the DL instability [18–21]. However, the parameters of laser ablation flows in ICF are markedly different from those of slow combustion. One of the most distinctive features of deflagration in ICF is that the plasma velocity reaches the isothermal sound speed at the critical surface of laser light absorption. Laser ablation corresponds to the so-called Chapman-Jouguet deflagration, which is the fastest propagation regime possible for a deflagration front. Another important property inherent to the plasma flow is the strong temperature dependence of thermal conduction, which determines the internal structure of laser deflagration. It is expected that the strong plasma compression and the thermal conduction will significantly influence the DL instability in a laser-generated plasma. There was much interest in the DL instability in ICF, e.g., see [8,11–16]. Still, these papers did not answer the following most important questions concerning the DL instability in laser ablation:

(1) How strong is the DL instability in laser ablation in comparison to the classical case, i.e., is it stronger or weaker than the DL instability developing at a slow flame front?

(2) What is the characteristic length scale of the instability development? This question is especially important from the experimental point of view, since the answer determines the target size, for which the DL instability may be observed.

(3) What is the outcome of the DL instability at the nonlinear stage?

A number of papers tried to answer the first question within the model of a discontinuous ablation front [10,11,16,30,31]. Unfortunately, the discontinuous model encounters the deficit of matching conditions at the front [3,5,9,16]; the solution to the problem turned out to be sensitive to this assumed extra condition. Unlike that, Refs. [32,33] took into account a continuous structure of the deflagration front in a compressible flow, thus eliminating the deficit of the matching conditions. Though Refs. [32,33] were devoted to combustion, and the respective results cannot be extrapolated directly to the DL instability in laser ablation, still the method used in these papers may be used for the ablation studies.

Here we employ the methods of Refs. [32,33] to study the linear stage of the DL instability in a laser plasma, thus answering questions 1 and 2 of those outlined above. We find the dispersion relation of the instability numerically as a solution to an eigenvalue stability problem taking into account the continuous structure of the flow. We demonstrate that the DL instability in laser ablation is much stronger than in the classical case of a usual slow flame. The characteristic length scale of the DL instability in the ablation flow is comparable

to the total distance from the ablation zone to the critical zone of laser light absorption.

II. BASIC EQUATIONS AND THE STATIONARY SOLUTION

We study the ablation plasma flow using hydrodynamic equations of mass, momentum, and energy conservation,

$$\frac{\partial \rho}{\partial t} + \nabla \cdot (\rho \mathbf{u}) = 0, \tag{1}$$

$$\rho \frac{\partial \mathbf{u}}{\partial t} + (\rho \mathbf{u} \cdot \nabla)\mathbf{u} + \nabla P = 0, \tag{2}$$

$$\frac{\partial}{\partial t}\left(\rho C_V T + \frac{1}{2}\rho u^2\right) + \nabla \cdot \left[\rho \mathbf{u}\left(C_P T + \frac{1}{2}u^2\right) - \kappa \nabla T\right] = \Omega_R, \tag{3}$$

and the equation of state of an ideal gas

$$P = \frac{\gamma - 1}{\gamma} C_P \rho T, \tag{4}$$

where $\gamma = 5/3$ is the adiabatic exponent, C_P and C_V are the heat capacities at constant pressure and volume, respectively. We describe plasma within the one-fluid approximation using the ideal gas equation with single temperature. This is a traditional approach to study hydrodynamic instabilities in ICF employed in the absolute majority of works on the subject, e.g., see [2–17]. Though simple, it captures all essential physics of the problem. Of course, one can always make the model more complicated by including specific details of laser-induced plasma medium [2]. For example, characteristic densities of heavy cold plasma of the target are comparable to solid-state density. It is questionable if such a plasma may be described by the ideal gas law. However, the flow of cold heavy plasma developing because of the DL instability may be treated as incompressible with a very good accuracy. An incompressible flow does not depend on a particular type of the equation of state of the moving medium. For this reason, we may employ the ideal gas law for the cold plasma without changing the physical results for the DL instability. Another possible complication is related to nonequilibrium electron distribution in the region of laser light absorption [2]. For high laser irradiance, two (or more) types of electrons are produced: "cold" and "hot." The cold electrons carry energy away from the point of absorption by the diffusion process (thermal conduction). The hot electrons deposit their energy faster causing electron preheating. A particular type of heat transfer within the deflagration (laser ablation) wave determines total thickness of the wave, and as a consequence, the characteristic length scale of the DL instability. One may also consider other types of thermal conduction in laser ablation such as black-body radiation flux [2,6,7], a complex combination of electron and/or radiation heat transfer, or flux-limited heat flow [11,29]. Influence of a particular type of heat transfer on the parameters of the DL instability is a complicated problem, which requires a separate study including the multifluid approximation of laser plasma. Such a study is beyond the scope of the present paper; otherwise the present work becomes too large and difficult for reading. Here we consider only the single-fluid approach; we investigate mostly the regime of electron thermal conduction with brief discussion on how the physical results are modified for other types of thermal conduction. Particularly, we show in Sec. IV that the scaled cutoff wavelength of the DL instability becomes noticeably shorter for stronger temperature dependence of thermal conduction.

Electron thermal conduction κ depends on temperature as $\kappa = \kappa_c (T/T_c)^{5/2}$, where label "c" refers to the critical surface of laser light absorption. Laser light absorption brings energy into the plasma and, together with thermal conduction, it drives the flow. Absorption takes place when plasma frequency is equal to the laser frequency $\omega_{\text{laser}}^2 = \omega_p^2 = e^2 \rho_c / \varepsilon_0 m_e M$, which determines plasma density ρ_c at the critical surface (here M is plasma mass per one electron). Decrease in the laser light intensity due to absorption may be described as $dI/dz = KI$ with the absorption coefficient [2]

$$K \propto \frac{\rho^2}{T^{3/2}}\left(1 - \frac{\rho}{\rho_c}\right)^{-1/2}. \tag{5}$$

The absorption coefficient diverges at the critical surface, and, therefore, the process of energy absorption is strongly localized at the surface. In the studies of ablation instabilities, the energy release is typically presented by δ function [3,5,10,11,28]. Such replacement is possible since the instabilities develop on the length scales much larger than the region of energy release and involve bending of this region as a whole without changing its internal structure. In the present paper we solve the problem of the DL instability numerically. In the numerical solution, it is more convenient to imitate the δ function by a transitional zone of finite width determined by some continuous function Ω_R of energy gain included into Eq. (3). Here, we chose the function in the form suggested in Ref. [16],

$$\Omega_R = \Omega(\rho - \rho_c)^n \exp(-\beta \rho / \rho_c). \tag{6}$$

The function Ω_R was constructed taken into account similarity with the Arrhenius law in combustion, where β plays the role of the scaled activation energy and n is similar to the reaction order. In combustion science the Arrhenius reaction is sensitive to temperature changes [19,20]. Here we construct the function of energy gain Ω_R sensitive to density variations, as it takes place in laser ablation. Choosing large parameter $\beta \to \infty$ we obtain energy gain strongly localized at the critical surface for $\rho \to \rho_c$. In most of our calculations we use $\beta = 90$, $n = 2$. We also checked that these parameters have minor influence upon the properties of the DL instability at sufficiently large values of β. The function Ω_R given by Eq. (6) allows a planar stationary solution consisting of two uniform flows of cold heavy plasma (label "a") and hot light plasma (label "c") separated by a transitional region, which is the deflagration front. The labels a and c originate from the ablation and critical surfaces in the laser deflagration. Typical internal structure of the deflagration front is illustrated in Fig. 1. The described geometry is common in the theoretical

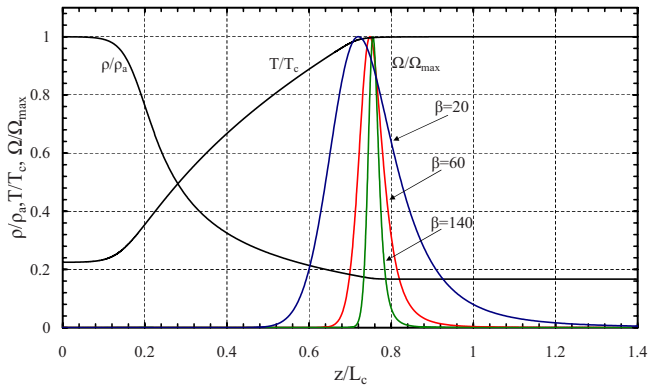

FIG. 1. (Color online) Profiles of density, temperature and energy release for $\Theta=6$, $\mathrm{Ma}_c=0.5$, $\beta=20,60,140$.

studies of the RT and DL instabilities of the ablation flow [3–6,8–11,31], though it does not take into account the rarefaction wave in the hot light plasma beyond the critical surface. As the main advantage of such a choice, we may consider different values of the Mach number in the light plasma, which would be impossible with a rarefaction wave. Changing the Mach number, we can go over continuously from the case of classical incompressible DL instability of a usual flame front to the case of laser ablation with ultimately strong plasma compression.

Figure 1 illustrates plasma density, temperature, and energy release in the planar stationary deflagration flow obtained numerically as described in the Appendix. The deflagration front in Fig. 1 propagates to the left with constant velocity U_a (the ablation velocity) in the negative direction of z axis. Velocity of a usual flame is determined by the rate of energy release and thermal conduction. Ablation velocity is determined by the critical density and the laser light intensity [28]. We adopt the reference frame of the deflagration front. In that case the front is at rest, but the cold heavy plasma flows to the right with uniform velocity $u_z=U_a$, undergoes transition in density and temperature in the deflagration wave, and, finally, the hot light plasma gets drifted away with uniform velocity $u_z=U_c$.

Equations of mass and momentum transfer (1) and (2) may be integrated for the planar stationary deflagration as

$$\rho u_z = \rho_a U_a = \rho_c U_c, \tag{7}$$

$$P + \rho u_z^2 = P_a + \rho_a U_a^2 = P_c + \rho_c U_c^2. \tag{8}$$

One of the main dimensionless parameters in the problem is the expansion factor

$$\Theta = \frac{\rho_a}{\rho_c} = \frac{U_c}{U_a}, \tag{9}$$

which shows density drop from the original cold plasma to the critical surface. Both in flames and laser ablation, the expansion factor is large: here we take $\Theta=5-12$, similar to [7,20]. In the case of ablation flow, the laser light frequency determines the critical density and the expansion factor. The other important parameter is the Mach number in the light plasma (gas) corresponding to the adiabatic sound,

$$\mathrm{Ma}_c = U_c \sqrt{\frac{\rho_c}{\gamma P_c}}. \tag{10}$$

The Mach number is negligible in the classical case of usual flames. In laser ablation, the isothermal Mach number is equal unity $\rho_c U_c^2/P_c=1$ in the light plasma, and we have $\mathrm{Ma}_c^2=1/\gamma$ for the adiabatic Mach number. In the present work we consider a general case of a deflagration front with an arbitrary Mach number changing within the limits $0 \le \mathrm{Ma}_c^2 < 1/\gamma$. The internal structure of the deflagration front follows from the stationary equation of energy transfer,

$$\frac{d}{dz}\left[\rho_c U_c\left(C_P T + \frac{1}{2}u^2\right) - \kappa\frac{dT}{dz}\right] = \Omega_R. \tag{11}$$

Characteristic width of the front is determined by thermal conduction in the hot region,

$$L_c \equiv \frac{\kappa_c}{C_p \rho_c U_c}. \tag{12}$$

The problem involves one more parameter of length dimension,

$$L_a \equiv \frac{\kappa_a}{C_p \rho_a U_a} = \frac{\kappa_a}{C_p \rho_c U_c}, \tag{13}$$

related to thermal conduction in the cold flow. Because of the strong temperature dependence of electron thermal conduction, these two length scales are quite different $L_c/L_a=(T_c/T_a)^{5/2}$. For example, for the temperatures ratio $T_c/T_a=6$, the length scales differ by two orders of magnitude $L_c/L_a \approx 88$. The strong difference in these length scales is one of the specific features of laser ablation in comparison with usual flames.

The relation between temperature and density in a deflagration flow follows from Eqs. (7) and (8),

$$\frac{T}{T_c} = (1+\gamma \mathrm{Ma}_c^2)\frac{\rho_c}{\rho} - \gamma \mathrm{Ma}_c^2\left(\frac{\rho_c}{\rho}\right)^2. \tag{14}$$

In the incompressible limit of usual flames, $\mathrm{Ma}_c^2 \ll 1$, this relation is reduced simply to $\rho T=const$, so that temperature ratio is determined by the expansion ratio, $T_c/T_a=\Theta$. In the case of strong gas compression, these two values differ considerably. For example, in the case of laser ablation with the critical Mach number $\mathrm{Ma}_c^2=1/\gamma$, we find from Eq. (14) that

$$\frac{T_c}{T_a} = \frac{\Theta^2}{2\Theta - 1}. \tag{15}$$

For high values of density drop, $2\Theta \gg 1$, temperature ratio is about twice smaller than the expansion factor, $T_c/T_a \approx \Theta/2$. Because of the reduced temperature ratio, the effect of two different length scales Eqs. (12) and (13) in the ablation flow is expected to become weaker than in a similar incompressible flow. With temperature ratio changing from $T_c/T_a=\Theta$ in the incompressible case to $T_c/T_a \approx \Theta/2$ in the ablation flow, we find the ratio of length scales $L_c/L_a=(T_c/T_a)^{5/2}$ decreasing by the factor of $(2)^{5/2} \approx 5.7$, which makes the density profile smoother.

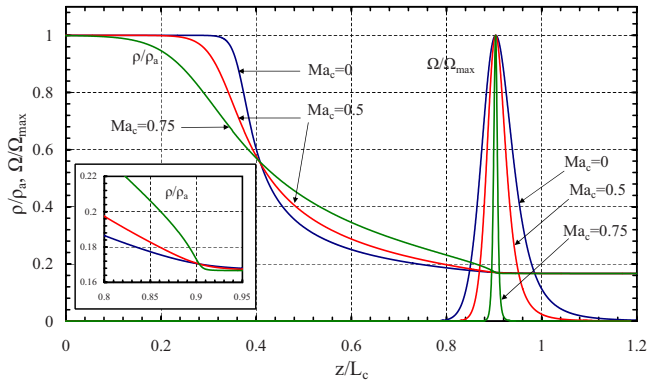

FIG. 2. (Color online) Profiles of density and energy release for different Mach numbers $\Theta=6$, $\mathrm{Ma}_c=0,0.5,0.75$.

In the numerical solution we have to make sure that the ablation front structure is not sensitive to our choice of the energy gain function Ω_R. We solve Eq. (11) together with Eq. (14) numerically for different values of parameter $\beta=20,60,140$, other parameters are $\Theta=6$, $n=2$, $\mathrm{Ma}_c=0.5$ (see Fig. 1). Density and temperature profiles for these three values of β almost coincide, so that the flow parameters do not depend on β. For $\beta\geq 90$, the width of the energy release takes less than 5% of the total thickness of the deflagration front. The other parameter of the energy gain function in Eq. (6), n, affects the shape of the energy release peak only slightly. Thus, Eq. (6) may imitate the energy gain in the ablation flow quite well; in the following we take $\beta=90$ and $n=2$.

We also solve Eq. (11) for different values of the Mach number $\mathrm{Ma}_c=0,0.5,0.75$ (see Fig. 2). In the case of incompressible flow, $\mathrm{Ma}_c=0$, the density profile demonstrates clearly the effect of two length scales, Eqs. (12) and (13), produced by the temperature-dependent thermal conduction. The profile is rather smooth in the hot region close to the critical surface, and it becomes sharp in the cold plasma close to the ablation surface. In the case of strong compression with $\mathrm{Ma}_c=0.75$, the density profile becomes much smoother, as discussed above, because of the reduced temperature difference T_c/T_a. Another specific feature of the density profile is shown at the inset of Fig. 2. With the Mach number approaching the maximal possible value $\mathrm{Ma}_c^2=1/\gamma$, we observe development of another miniregion of relatively high density gradient close to the critical surface. This effect may be also obtained analytically from Eq. (14). Close to the critical surface, expanding density and temperature in power series with respect to $\rho/\rho_c-1\ll 1$, $1-T/T_c\ll 1$, we obtain the relation $\rho/\rho_c-1\approx\sqrt{1-T/T_c}$. Taking energy gain in the form of δ function, we have temperature achieving the final value T_c at finite point $z=0$ smoothly. This leads to the square-root singularity in the density gradient. We can observe the trace of such a singularity in the inset of Fig. 2, though smoothed because of the finite width of the energy gain zone. For the same reason, the energy gain zone becomes much thinner at high values of the Mach number. Since the energy release Eq. (6) is sensitive to the density profiles, then sharp density gradients at $\mathrm{Ma}_c^2=1/\gamma$ make the zone of energy gain sharper as well. The numerical solution for the planar stationary flow provides the basis for the stability analysis.

III. LINEARIZED EQUATIONS

We solve the stability problem for small perturbations of any value ϕ in the form: $\phi(x,z,t)=\phi(z)+\tilde{\phi}(z)\exp(\sigma t+ikx)$, where the first term stands for the stationary flow, the second term describes linear perturbations, σ is the instability growth rate, and $k=2\pi/\lambda$ is the perturbation wave number. In general, σ may have both a real part (growth rate) and an imaginary part (frequency). However, in the case of the DL instability σ is only real; the instability develops when σ is positive.

The linearized system (1)–(3) takes the form

$$\sigma\tilde{\rho}+\frac{d}{dz}(\rho\tilde{u}_z+\tilde{\rho}u_z)+ik\rho\tilde{u}_x=0, \tag{16}$$

$$\sigma\rho\tilde{u}_x+\rho u_z\frac{d\tilde{u}_x}{dz}+ik\tilde{P}=0, \tag{17}$$

$$\sigma\rho\tilde{u}_z+\rho u_z\frac{d\tilde{u}_z}{dz}+\frac{du_z}{dz}(\tilde{\rho}u_z+\rho\tilde{u}_z)+\frac{d\tilde{P}}{dz}=0, \tag{18}$$

$$\sigma(\rho C_V\tilde{T}+\rho u\tilde{u}-\tilde{\rho}RT)+(\tilde{\rho}u_z+\rho\tilde{u}_z)\frac{\partial}{\partial z}\left(C_PT+\frac{1}{2}u^2\right)+\rho u_z\frac{\partial}{\partial z}(C_P\tilde{T}+u\tilde{u})+\frac{\kappa_c}{T_c^{5/2}}\left[k^2T^{5/2}\tilde{T}-\frac{\partial}{\partial z}\left(\frac{5}{2}\frac{\partial T}{\partial z}\tilde{T}+T\frac{\partial\tilde{T}}{\partial z}\right)\right]-\tilde{\Omega}_R=0. \tag{19}$$

As the boundary conditions, we demand that perturbations vanish at infinity in the uniform flows of cold plasma ahead of the ablation zone and the hot plasma behind the critical zone of energy gain. The coefficients in Eqs. (16)–(19) are constant in the uniform flows. This allows us writing down the perturbations in an exponential form $\tilde{\phi}(z)=\tilde{\phi}\exp(\mu z/L_c)$, where $\mu>0$ in the heavy plasma ($z\to-\infty$) and $\mu<0$ in the light plasma ($z\to\infty$). In some particular simplified limits the structure of the perturbation modes in the uniform flows may be written analytically, e.g., see [16]. However, in the present case we can do it only numerically, see Appendix.

Strictly speaking, a uniform flow of light heated plasma is only a model for laser ablation, which is typically used in the studies of the RT and DL instabilities [3–6,8–11]. Instead, light plasma expands into vacuum in the form of a rarefaction wave, which is intrinsically time dependent [28,29]. It is commonly assumed that replacement of the rarefaction wave by a uniform flow does not influence the instability development. However, it is not easy to prove this rigorously. Only few recent papers considered the RT instability in laser ablation taking into account time-dependent self-similar nature of the unperturbed flow [34,35]. This task requires a separate large work, which is beyond the scope of the present paper and which we leave for future studies. Besides, without using the model of a uniform flow of light plasma, we cannot go over continuously from the limit of usual slow flame to laser

ablation. We stress that comparison of these two asymptotic cases of negligible and ultimately strong plasma compression is the main purpose of the present work.

IV. RESULTS AND DISCUSSION

Before presenting the numerical solution to the stability problem, we explain the physical results we are looking for. In the classical case of an infinitely thin flame front propagating in an incompressible flow, the instability growth rate was obtained by Darrieus and Landau [18,19] as

$$\sigma = \Gamma U_a k, \tag{20}$$

where the coefficient Γ depends on the expansion factor Θ only,

$$\Gamma = \frac{\Theta}{\Theta+1}\left(\sqrt{\Theta+1-1/\Theta}-1\right). \tag{21}$$

Taking into account gas compression, we should expect the dispersion relation for an infinitely thin deflagration front in the same form as Eq. (20), but with the coefficient Γ depending on the Mach number, $\Gamma=\Gamma(\Theta,\mathrm{Ma}_c)$. More general solution to the stability problem takes into account finite thickness of the deflagration front, which leads to stabilization of the DL instability at sufficiently short wavelengths. In the case of usual slow flames of finite thickness, the analytical solution to the problem may be found, e.g., in [21]. Written in the form of Taylor expansion in relatively small perturbation wave number, $kL_c \ll 1$, the solution may be presented as

$$\sigma = \Gamma U_a k(1 - k/k_{cut}), \tag{22}$$

where k_{cut} is the cutoff wave number, $\lambda_{cut}=2\pi/k_{cut}$ is the cutoff wavelength. The approximation of the small cutoff wave number $k_{cut}L_c \ll 1$ holds with reasonable accuracy for usual flames, e.g., see the review [20]. The cutoff wavelength is proportional to the thickness of the deflagration front, $\lambda_{cut} \propto L_c$. In the incompressible flow, the coefficient of proportionality depends on the expansion factor Θ and on the type of thermal conduction. Particularly, in the case of $\kappa \propto T^\nu$ and an incompressible flow, the theory [21] predicts

$$\frac{\lambda_{cut}}{L_c} = \frac{2\pi\Theta}{\nu(\Theta-1)}\left[(1-\Theta^{-\nu})\frac{\Theta+1}{\Theta-1} + \frac{1-\Theta^{-\nu-1}}{1+1/\nu}\right]. \tag{23}$$

For electron thermal conduction, $\nu=5/2$, and typical expansion factors $\Theta=6-8$, Eq. (23) predicts the cutoff wavelength $\lambda_{cut} \approx 6L_c$. In the case of radiation heat transfer, temperature dependence of thermal conduction is much stronger, as strong as $\kappa \propto T^{13/2}$ (see [2]). Then, for $\Theta=6-8$, the cutoff wavelength may be evaluated as $\lambda_{cut} \approx 2.5L_c$, which is considerably smaller than in the case of electron thermal conduction. According to Eq. (23), strong temperature dependence of thermal conduction, $\kappa \propto T^\nu$ with $\nu \gg 1$, reduces the scaled cutoff wavelength as $\lambda_{cut}/L_c \propto 1/\nu$. As an opposite case, thermal conduction is almost temperature independent for usual flames, and the scaled DL cutoff is much larger, being about $\lambda_{cut}/L_c \approx 20$ (see [20]). According to the dispersion relation (22), there is a maximum of the instability growth rate $\sigma_{\max}$ achieved at a certain finite perturbation wavelength $\lambda_{\max}$. Equation (22) predicts the wavelength of the maximum to be twice larger than the cutoff wavelength, $\lambda_{\max}=2\lambda_{cut}$. Taking into account gas compression, one should expect that all these values depend on the Mach number, Ma_c. Therefore, the purpose of the present work is to investigate dependence of the parameters Γ, λ_{cut}, $\lambda_{\max}$, and $\sigma_{\max}$ on the Mach number Ma_c changing within the interval $0<\mathrm{Ma}_c<1/\sqrt{\gamma}$. We demonstrate below that this dependence is quite strong.

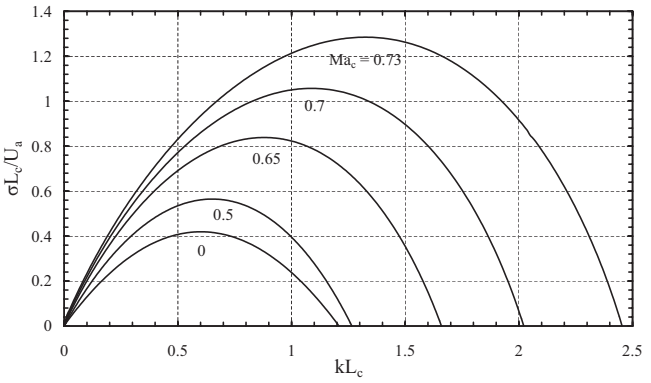

FIG. 3. Scaled instability growth rate versus the scaled wave number for different Mach numbers and $\Theta=6$.

Figure 3 presents the scaled instability growth rate obtained numerically versus the perturbation wave number. The dispersion relation is shown for different values of the Mach number, $\mathrm{Ma}_c=0-0.73$, with the expansion factor $\Theta=6$. The DL instability becomes much stronger with increasing the Mach number, which concerns all parameters of the instability. Figure 4 shows the factor Γ characterizing strength of the DL instability at an infinitely thin front. In that case, the DL instability is almost twice stronger for laser ablation than in the incompressible flow. The factor Γ is also noticeably larger than any analytical theory predicted so far (see [10,11,16,30,31]). As explained in [16], the analytical theories employed the model of a discontinuous ablation front suffering from the deficit of matching conditions at the front. This trouble does not happen in the present numerical solution, which may also help in constructing the analytical

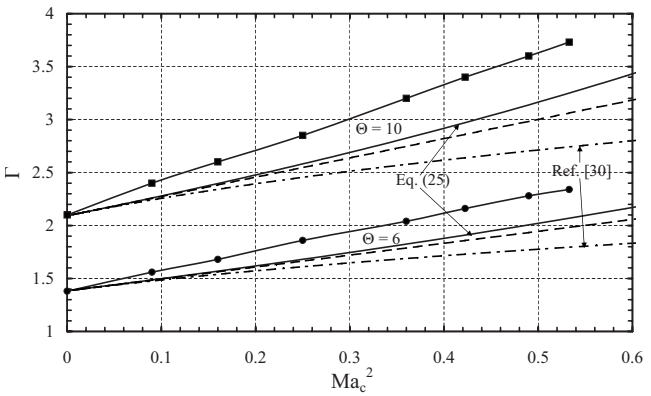

FIG. 4. The Γ factor versus the Mach number squared for $\Theta=6$ (circles) $\Theta=10$ (squares). The solid lines depict Eq. (25), the dashed lines correspond to Eq. (28), the dash-dotted lines present the result of Ref. [30].

theory. Here we will try to extract the best ideas suggested so far in [10,11,16,30,31] to obtain the analytical solution reasonably close to the numerical one. For that purpose we take the basic elements in the analysis [16] and complement them by an extra condition identical to that of the classical DL theory [18] (see also [10,11,30]),

$$\tilde{u}_{za} - \frac{\partial f}{\partial \tau} = 0, \tag{24}$$

where f is perturbation of the discontinuous front position. Reproducing calculations of [16] with the extra condition (24) we obtain the following equation for Γ:

$$\frac{1-(2\Theta-1)\mathrm{Ma}_a^2}{1-\Theta\mathrm{Ma}_a^2}\frac{\Gamma\eta_c-1}{\Gamma-\eta_c}(\Theta\Gamma+\eta_a)+\Gamma\eta_a+1 - \frac{\Theta-1}{\Theta\Gamma}\frac{\eta_a+\Theta^2\mathrm{Ma}_a^2\Gamma^3}{1-\Theta\mathrm{Ma}_a^2}=0, \tag{25}$$

where

$$\eta_a=\sqrt{1+\mathrm{Ma}_a^2(\Theta^2\Gamma^2-1)}, \quad \eta_c=\sqrt{1+\mathrm{Ma}_c^2(\Gamma^2-1)} \tag{26}$$

and the Mach number in the cold plasma

$$\mathrm{Ma}_a^2=\frac{\mathrm{Ma}_c^2}{\Theta+\gamma(\Theta-1)\mathrm{Ma}_c^2}. \tag{27}$$

Influence of the Mach number may be illustrated in the limit of small plasma compression, $\mathrm{Ma}\ll 1$, using Taylor expansion of Eq. (25). In that case

$$\Gamma=\Gamma_0(1+\varepsilon\mathrm{Ma}_c^2), \tag{28}$$

where Γ_0 corresponds to DL solution for incompressible case, Eq. (21), and ε is determined as

$$\varepsilon=1-\frac{2\Theta[\Gamma_0(\Theta+2)+1]}{(\Theta+1)^2[\Gamma_0(\Theta+1)+\Theta]}>0. \tag{29}$$

Positive factor ε indicates increase in the instability growth rate with compression effects. The solutions to Eq. (25) together with Eq. (28) are presented in Fig. 4 by the solid and dashed lines, respectively. These lines do not provide a perfect agreement with the numerical results; still the difference between the theory and the numerical solution is acceptable, about 15%. For comparison, Fig. 4 shows also the instability growth rate predicted in [30], by dash-dotted lines. The theory in [30] differs much stronger from the numerical solution, approximately by 35%.

Figure 5 shows the maximal instability growth rate versus the Mach number for the expansion factors $\Theta=6,10$, and electron thermal conduction $\nu=5/2$. In the case of laser ablation with $\mathrm{Ma}_c=1/\sqrt{\gamma}$ the maximal instability growth rate is about three times larger than in the incompressible case. These results agree well with the previous numerical calculations of Ref. [32] for flames in a compressible flow. It is interesting that the maximal growth rate shows only minor dependence on the Mach number for a rather wide range of this parameter, $\mathrm{Ma}_c<0.5$. The strong increase in $\sigma_{\max}$ with Ma_c takes place only when the Mach number starts approaching the limiting value $\mathrm{Ma}_c=1/\sqrt{\gamma}$ inherent to laser ablation. Besides we have calculated the same value for radiation energy transport, corresponding to $\nu=13/2$. It behaves qualitatively in a similar way but the instability growth rate is almost three times larger for radiation thermal conduction in comparison with the electron one. We observe the same tendency in Fig. 6, which presents the cutoff wavelength versus the Mach number. For $\nu=13/2$ the cutoff wavelength also decreases considerably. Figure 7 compares the cutoff wavelength found numerically for different values of the Mach number to the theoretical prediction Eq. (23) for $\nu=5/2$. The theory (23) provides a reasonable prediction for the cutoff wavelength in the case of zero Mach number; the difference between the theory and the numerical solution is about (15–25)%. As we increase the Mach number, the DL instability becomes stronger and the cutoff wavelength decreases considerably. For example, taking the expansion ratio $\Theta=7$ we find the cutoff wavelength $\lambda_{cut}\approx 2.4L_c$ for laser ablation, $\lambda_{cut}\approx 4.8L_c$ for the incompressible case of $\mathrm{Ma}_c=0$ and $\lambda_{cut}\approx 6L_c$ predicted by the analytical formula (23) for electron thermal conduction. The cutoff wavelength, $\lambda_{cut}\approx 2.4L_c$, is very small when compared to the respective value, $\lambda_{cut}/L_c\approx 20$, for usual flames. However, it is extremely large in comparison with the length scales typical for the RT instability in ICF [5,6,8]. Experimental observations typically concern the fastest growing perturbations of the wavelength $\lambda_{\max}$ and larger, not the cutoff wavelength. In the

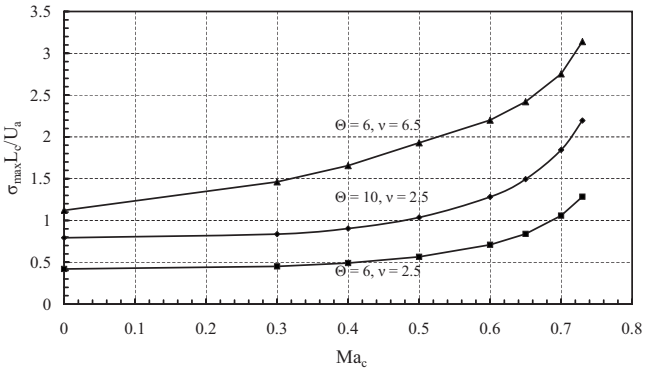

FIG. 5. Maximum of scaled instability growth rate versus the Mach number for $\Theta=6,10$, $\nu=2.5,6.5$.

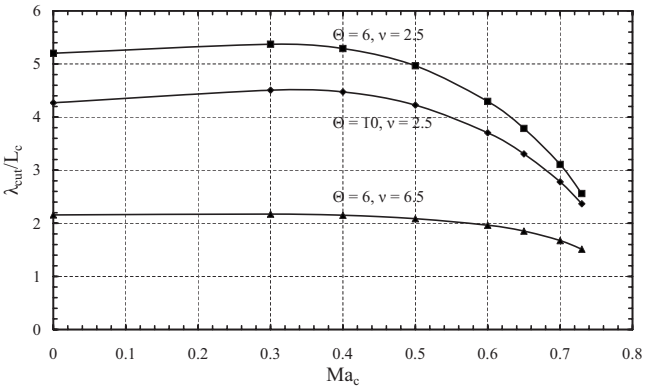

FIG. 6. The cutoff wavelength versus the Mach number, $\Theta=6,10$, $\nu=2.5,6.5$.

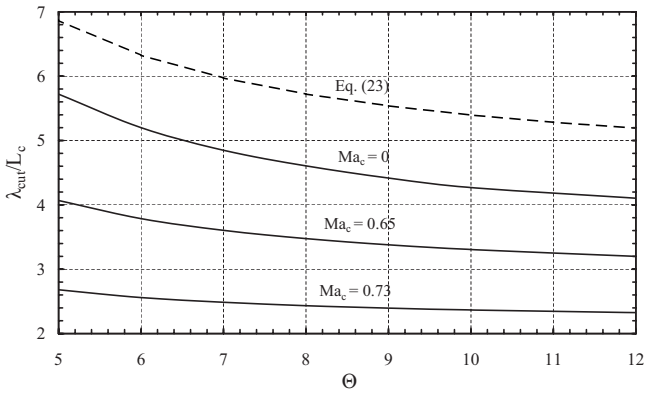

FIG. 7. The cutoff wavelength versus the expansion factor for $\mathrm{Ma}_c=0,0.65,0.73$. The dashed line shows the analytical formula Eq. (23).

case of usual flames these two length scales are related as $\lambda_{\max}/\lambda_{cut}\approx 2$ [see Eq. (22)]. This ratio becomes somewhat different for the DL instability in laser ablation, $\lambda_{\max}/\lambda_{cut}\approx 1.8$.

Finally, we give an example of experimental plasma parameters needed to observe the DL instability in laser ablation. Both the RT and DL instabilities behave in a similar way bending the ablation front, and they require similar diagnostics. For this reason, when designing the experiment one has to be sure that the DL instability dominates over the RT instability, at least at the perturbation wavelengths about $\lambda_{\max}$. As an example, we take an ablation flow similar to Ref. [7] with the expansion factor $\Theta=6$, which provides the DL instability of about same strength as in the present numerical calculations. We consider a DT target with initial density $\rho_a=0.2$ g/cm^3, ablation velocity $U_a=3.5$ μm/ns, ablation front thickness $L_a=0.18$ μm, and Spitzer electron thermal conduction with $\nu=5/2$. The required laser wavelength may be found from the relation between the critical density $\rho_c=\rho_a/\Theta$ and the laser frequency, $\omega_{\mathrm{laser}}=e\sqrt{\rho_c/\varepsilon_0 m_e M}$, see Sec. II, which in the present case leads to $\lambda_{\mathrm{laser}}\approx 0.45$ μm. The theory [2,28,29] yields the laser intensity $I_{\mathrm{laser}}\approx 5\times 10^{13}$ W/cm^2 needed to produce such a flow, which is in line with recent experiments [13,14,36]. We can also find the distance to the critical surface in such a flow as $L_c=\Theta^{\nu}L_a\approx 16$ μm and the wavelength of the fastest growing DL perturbations $\lambda_{\max}=74$ μm using Fig. 6. From Fig. 5, we find the respective maximal DL instability growth rate $\sigma_{\max}\approx 0.3$ ns^{-1}, which is an order of magnitude smaller than the RT growth rate encountered in similar experimental flows, e.g., see [36,37]. Still, the RT instability depends on the target acceleration g and on the initial target size L_{target}, since $g\approx P_a/\rho_a L_{\mathrm{target}}$, where ablation pressure is determined by Eq. (8). The RT instability growth rate decreases for large targets as $\sigma_{\mathrm{RT}}\propto\sqrt{gk}\propto 1/\sqrt{L_{\mathrm{target}}}$. On the contrary, the DL instability does not depend on the acceleration and we can find the target size for which the ablative DL instability dominates. Evaluating the RT instability growth rate from above by $\sigma_{\mathrm{RT}}\leq\sqrt{gk}$, we find that a target of thickness $L_{\mathrm{target}}=2\times 10^3$ μm provides the DL instability about five times stronger than the RT instability. Such a large target is unusual for ablation experiments, but it allows observing the DL instability. Taking larger targets we make the relative role of the DL instability even stronger. Still, all these estimates depend strongly on the expansion factor Θ and on the type of thermal conduction. For example, using data of Ref. [37] for a DT target with the laser intensity $I_{\mathrm{laser}}=10^{14}$ TW/cm^2, laser wavelength $\lambda_{\mathrm{laser}}=0.35$ μm, and the thermal conduction exponent $\nu=2.1$, we find a noticeably higher expansion factor as $\Theta\approx 40$. Then we calculate the corresponding distance to the critical surface $L_c\approx 170$ μm and the wavelength of the fastest DL perturbations $\lambda_{\max}\approx 450$ μm. In such an experiment, to obtain $\sigma_{\max}$ for the DL instability about five times greater than $\sqrt{gk}$ one has to use targets as large as $L_{\mathrm{target}}\approx 1.3\times 10^4$ μm. For comparison, experiments [37] on the RT instability were performed for targets two orders of magnitude smaller, $L_{\mathrm{target}}=1.9\times 10^2$ μm. Flow parameters change even more dramatically if the radiative thermal conduction (with $\nu=13/2$) dominates over the electron one. Therefore, in designing an experiment on the ablative DL instability one has to study accurately the thermal conduction mechanism of the plasma flow, since the instability parameters depend strongly on it.

V. CONCLUSIONS

In the present paper we investigated the DL instability in an ablation flow and compared the results to the classical case of a slow flame. Unlike the normal flame, laser ablation is characterized by the strongest plasma compression possible for a deflagration wave. Another specific feature of laser ablation is the strong dependence of thermal conduction on temperature. We demonstrate that the DL instability in laser ablation is much stronger than in the classical case. In particular, the maximal growth rate in the ablation flow is about three times larger than in the incompressible case. Moreover, the cutoff wavelength changes drastically as we go from the classical case of an incompressible flow to the ablation flow. The cutoff wavelength is also strongly influenced by the temperature dependence of thermal conduction. It is known that the DL instability for usual flames develops on quite large length scales exceeding the flame thickness by almost two orders of magnitude [20]. In contrast to this, the characteristic length scale of the DL instability in the ablation flow (e.g., the cutoff wavelength) is comparable to the total distance from the ablation zone to the critical zone of laser light absorption, L_c. Still, even these values are large from the point of view of possible experimental observations of the DL instability in laser ablation. We note that the RT instability in inertial confined fusion develops on length scales much smaller than L_c. For this reason, the DL instability may be observed only if the accompanied RT instability is suppressed. This may be achieved, for example, for sufficiently large targets of thickness much larger than the distance L_c from the critical to the ablation zone.

ACKNOWLEDGMENTS

This work was supported by the Swedish Research Council and by the Kempe foundation.

APPENDIX: THE NUMERICAL METHOD

In the numerical solution, we introduce dimensionless variables for plasma density, temperature, and velocity, and coordinate $\varphi=\rho/\rho_c$, $\theta=T/T_c$, $u=u_z/U_c$, and $\xi=z/L_c$. Then we can rewrite Eq. (11) as

$$\frac{\partial}{\partial\xi}\left[\theta+\frac{(\gamma-1)}{2\varphi^2}\mathrm{Ma}_c^2-\theta^{5/2}\frac{\partial\theta}{\partial\xi}\right]=\Lambda(\varphi-1)^n\exp(-\beta\varphi), \tag{A1}$$

where $\Lambda=L_c^2\Omega\rho_c^n(\kappa_cT_c)^{-1}$ is an eigenvalue of the stationary problem.

In the linearized problem, Eq. (16)–(19) we introduce the dimensionless perturbations of mass flow $\tilde{j}$, transverse velocity $\tilde{v}$, temperature $\tilde{\theta}$, and dynamic pressure $\tilde{\Pi}$ as

$$\tilde{j}=\frac{\rho\tilde{u}_z+\tilde{\rho}u_z}{\rho_cu_c},\quad \tilde{v}=\frac{i\tilde{u}_x}{u_c},\quad \tilde{\theta}=\frac{\tilde{T}}{T_c},\quad \tilde{\Pi}=\frac{\tilde{P}+\tilde{\rho}u_z^2+2\rho u_z\tilde{u}_z}{\rho_cu_c^2} \tag{A2}$$

with the scaled wave number and the perturbation growth rate $K=kL_c$, $S=\sigma L_c/U_c$. We also introduce an auxiliary variable $\psi=\theta^{5/2}\partial\theta/\partial\xi$, which corresponds to the heat flux with a respective linearized value. Then the linearized system (16)–(19) is

$$\frac{d\tilde{j}}{d\xi}=2S\frac{\gamma\mathrm{Ma}_c^2u}{w}\tilde{j}-K\varphi\tilde{v}-S\frac{\gamma\mathrm{Ma}_c^2}{w}\tilde{\Pi}+S\frac{\varphi}{w}\tilde{\theta}, \tag{A3}$$

$$\frac{d\tilde{v}}{d\xi}=-2K\frac{\theta u}{w}\tilde{j}-S\varphi\tilde{v}+K\frac{\theta}{w}\tilde{\Pi}-K\frac{u}{w}\tilde{\theta}, \tag{A4}$$

$$\frac{d\tilde{\Pi}}{d\xi}=-S\tilde{j}-K\tilde{v}, \tag{A5}$$

$$\frac{d\tilde{\theta}}{d\xi}=-\frac{5}{2}\frac{1}{\theta}\frac{d\theta}{d\xi}\tilde{\theta}+\theta^{-5/2}\tilde{\psi}, \tag{A6}$$

$$\frac{\partial\tilde{\psi}}{\partial\xi}=A_j\tilde{j}+A_v\tilde{v}+A_\Pi\tilde{\Pi}+A_\theta\tilde{\theta}+A_\psi\tilde{\psi}, \tag{A7}$$

where $w=\theta-\gamma\mathrm{Ma}_c^2u^2$ and the coefficients in Eq. (A6) and (A7) are

$$A_j=\frac{\partial\theta}{\partial\xi}+(\gamma-1)\mathrm{Ma}^2\left[\frac{u}{w}\left(S(3\theta+\gamma\mathrm{Ma}^2u^2)\frac{\theta}{w}+\frac{2\gamma}{\gamma-1}\frac{\partial\Omega_R}{\partial\varphi}\right)+\frac{\partial}{\partial\xi}\left\{\frac{3\theta+\gamma\mathrm{Ma}^2u^2}{2w}u^2\right\}\right], \tag{A8}$$

$$A_v=(\gamma-1)\mathrm{Ma}_c^2\frac{u}{w}K\theta, \tag{A9}$$

$$A_\Pi=-(\gamma-1)\mathrm{Ma}_c^2\left[S\frac{\theta+\gamma\mathrm{Ma}_c^2u^2}{w^2}\theta+\frac{\gamma}{(\gamma-1)w}\frac{\partial\Omega_R}{\partial\varphi}+\gamma\mathrm{Ma}_c^2\frac{\partial}{\partial\xi}\left\{\frac{u^3}{w}\right\}\right], \tag{A10}$$

$$A_\theta=S\frac{\varphi\theta}{w}+K^2\theta^{5/2}+\frac{\partial\Omega_R}{\partial\varphi}\frac{\varphi}{w}-\frac{5}{2w}\frac{\partial\theta}{\partial\xi}+\mathrm{Ma}_c^2\left[\frac{5u^2}{2w\theta}\frac{\partial\theta}{\partial\xi}+S[(2\gamma-3)\theta+\gamma\mathrm{Ma}_c^2u^2]\frac{u}{w^2}+(\gamma-1)\frac{\partial}{\partial\xi}\left\{\frac{u^2}{w}\right\}\right], \tag{A11}$$

$$A_\psi=\theta^{-5/2}\frac{\theta-\mathrm{Ma}_c^2u^2}{w}. \tag{A12}$$

Thus we have a system of five differential equations of the first order with the scaled growth rate S as an eigenvalue. The purpose of the solution is to find the dispersion relation $S=S(K)$. The system may be written in a matrix form

$$\frac{\partial\tilde{\phi}}{\partial\xi}=\mathbf{F}\tilde{\phi}, \tag{A13}$$

where $\tilde{\phi}$ is a vector of the perturbations and $\mathbf{F}$ is the matrix

$$\mathbf{F}=\begin{bmatrix} 2S\frac{\gamma\mathrm{Ma}_c^2u}{w} & -K\varphi & -S\frac{\gamma\mathrm{Ma}_c^2}{w} & S\frac{\varphi}{w} & 0 \\ -2K\frac{\theta u}{w} & -S\varphi & K\frac{u}{w} & K\frac{\theta}{w} & 0 \\ -S & -K & 0 & 0 & 0 \\ 0 & 0 & 0 & -\frac{5}{2}\frac{1}{\theta}\frac{d\theta}{d\xi} & \theta^{-5/2} \\ A_j & A_v & A_\Pi & A_\theta & A_\psi \end{bmatrix}. \tag{A14}$$

Boundary conditions to Eq. (A13) are determined by modes $\tilde{\phi}(\xi)=\tilde{\phi}\exp(\mu\xi)$ in the uniform flows. In order to find the factors μ, we solve $|\mathbf{F}-\mathbf{E}\mu|=0$, where $\mathbf{E}$ is the unit matrix. The equation for μ is a polynomial of the fifth order. In the incompressible case this equation may be solved analytically. Five different roots correspond to the vorticity mode, two sound modes, and two modes of thermal conduction and/or energy gain [5,16,38]. In the case of a compressible flow, we find numerically five modes with two positive and three negative values taking $\mu>0$ for $\xi\to-\infty$ and $\mu<0$ for $\xi\to\infty$. Finally, we integrate the system (A13) numerically in the transitional region of the deflagration flow. We perform the numerical integration two times from the right-hand side and three times from the left-hand side with boundary conditions determined by different modes. We match these five solutions at a certain point between the maximum of the energy release and the ablation zone of sharp density gradients. The physical results do not depend on the choice of the matching point. Then we obtain a matrix consisting of twenty five values describing flow perturbations for five

modes. Taking the determinant of this matrix equal zero, we find the dispersion relation $S=S(K)$.

In the numerical solution, we also check that our model for the energy gain in the deflagration/laser ablation flow does not influence the physical results obtained. We investigated influence of the parameters β and n of the energy gain on the DL dispersion relation. Numerical calculations for $\beta=90$ and different values of n show negligible variations in all parameters of the instability: the Γ factor, the maximal instability growth rate, and the cutoff wavelength. We also took $n=2$ and varied β within the limits between 20 and 140. For example, taking $\mathrm{Ma}_c=0.65$ we find the maximal growth rate $\sigma_{\max}L_c/U_a=0.74$ for $\beta=20$, $\sigma_{\max}L_c/U_a=0.84$ for $\beta=90$, and $\sigma_{\max}L_c/U_a=0.86$ for $\beta=140$. These calculations indicate that the continuous numerical model for the energy gain function Ω_R in Eq. (6) brings inaccuracy of only few per cent, about 3%, into the numerical solution for $\beta=90$ used in the present paper. Investigation of the cutoff wavelength for different β and n leads to similar conclusions.

[1] M. Dunne, Nat. Phys. **2**, 2 (2006).
[2] S. Eliezer, *The Interaction of High-Power Lasers with Plasmas* (IOP, Bristol, 2002).
[3] S. Bodner, Phys. Rev. Lett. **33**, 761 (1974).
[4] H. Kull, Phys. Rep. **206**, 197 (1991).
[5] V. Bychkov, S. Golberg, and M. Liberman, Phys. Plasmas **1**, 2976 (1994).
[6] R. Betti, V. Goncharov, R. McCrory, and C. Verdon, Phys. Plasmas **2**, 3844 (1995).
[7] R. Betti and J. Sanz, Phys. Rev. Lett. **97**, 205002 (2006).
[8] J. Sanz, L. Masse, and P. Clavin, Phys. Plasmas **13**, 102702 (2006).
[9] V. Bychkov, M. Modestov, V. Akkerman, and L.-E. Eriksson, Plasma Phys. Controlled Fusion **49**, B513 (2007).
[10] A. Piriz, Phys. Plasmas **8**, 5268 (2001).
[11] A. Piriz and R. Portugues, Phys. Plasmas **10**, 2449 (2003).
[12] M. Keskinen, A. Velikovich, and A. Schmitt, Phys. Plasmas **13**, 122703 (2006).
[13] O. Gotchev, V. Goncharov, J. Knauer, T. Boehly, T. Collins, R. Epstein, P. Jaanimagi, and D. Meyerhofer, Phys. Rev. Lett. **96**, 115005 (2006).
[14] V. Goncharov, O. Gotchev, E. Vianello, T. Boehly, J. Knauer, P. McKenty, P. Radha, S. Regan, T. Sangster, S. Skupsy, R. Betti, R. McGrory, D. Meyerhofer, and C. Cherfils-Clerouin, Phys. Plasmas **13**, 012702 (2006).
[15] P. Clavin and L. Masse, Phys. Plasmas **11**, 690 (2004).
[16] V. Bychkov, M. Modestov, and M. Marklund, Phys. Plasmas **15**, 032702 (2008).
[17] M. Modestov, V. Bychkov, R. Betti, and L.-E. Eriksson, Phys. Plasmas **15**, 042703 (2008).
[18] L. Landau and E. Lifshitz, *Fluid Mechanics* (Pergamon, Oxford, 1989).
[19] Ya. Zeldovich, G. Barenblatt, V. Librovich, and G. Makhviladze, *Mathematical Theory of Combustion and Explosion* (Consultants Bureau, New York, 1985).
[20] V. Bychkov and M. Liberman, Phys. Rep. **325**, 115 (2000).
[21] G. Searby and P. Clavin, Combust. Sci. Technol. **46**, 167 (1986).
[22] B. Link, Phys. Rev. Lett. **68**, 2425 (1992).
[23] M. Kamionkowski and K. Freese, Phys. Rev. Lett. **69**, 2743 (1992).
[24] P. C. Fragile and P. Anninos, Phys. Rev. D **67**, 103010 (2003).
[25] V. Gamezo, A. Khokhlov, E. Oran, A. Chtchelkanova, and R. Rosenberg, Science **299**, 77 (2003).
[26] V. Bychkov and M. Liberman, Astron. Astrophys. **302**, 727 (1995).
[27] V. Bychkov, M. Popov, A. Oparin, L. Stenflo, and V. Chechetkin, Astron. Rep. **50**, 298 (2006).
[28] W. Manheimer, D. Colombant, and J. Gardner, Phys. Fluids **25**, 1644 (1982).
[29] R. Fabbro, C. Max, and E. Fabre, Phys. Fluids **28**, 1463 (1985).
[30] S. Kadowaki, Phys. Fluids **7**, 220 (1995).
[31] L. He, Europhys. Lett. **49**, 576 (2000).
[32] O. Travnikov, M. Liberman, and V. Bychkov, Phys. Fluids **9**, 3935 (1997).
[33] O. Travnikov, V. Bychkov, and M. Liberman, Phys. Fluids **11**, 2657 (1999).
[34] M. Murakami, T. Sakaiya, and J. Sanz, Phys. Plasmas **14**, 022707 (2007).
[35] J.-M. Clarisse, C. Boudesocque-Dubois, and S. Gauthier, J. Fluid Mech. **609**, 1 (2008).
[36] W. Hsing, Cris W. Barnes, J. Beck, N. Hoffman, D. Galmiche, A. Richard, J. Edwards, P. Graham, S. Rothman, and B. Thomas, Phys. Plasmas **4**, 1832 (1997).
[37] R. Betti, V. Goncharov, R. McCrory, and C. Verdon, Phys. Plasmas **5**, 1446 (1998).
[38] M. A. Liberman, V. V. Bychkov, S. M. Golberg, and D. L. Book, Phys. Rev. E **49**, 445 (1994).